Interseasonal Variations in the Middle Atmosphere Forced by Gravity Waves

H. G. Mayr[1], J. G. Mengel[2], D. P. Drob[3], H. S. Porter[4], and K. L. Chan[5]
[1] Goddard Space Flight Center, Greenbelt, MD, 20771
[2] Science Systems & Applications, Inc., Lanham, MD,
[3] Naval Research Laboratory, Washington, DC, 20375
[4] Furman University, Greenville, SC, 29613
[5] Hong Kong University of Science and Technology, Hong Kong, China

Prepared for Submission

to

Journal of Atmospheric and Solar Terrestrial Physics

April, 2002

Abstract. In our Numerical Spectral Model (NSM), which incorporates Hines' Doppler Spread Parameterization, gravity waves (GW) propagating in the east/west direction can generate the essential features of the observed equatorial oscillations in the zonal circulation and in particular the QBO extending from the stratosphere into the upper mesosphere. We report here that the NSM also produces inter-seasonal variations in the zonally symmetric (m = 0) meridional circulation. A distinct but variable meridional wind oscillation (MWO) is generated, which appears to be the counterpart to the QBO. With a vertical grid-point resolution of about 0.5 km, the NSM produces the MWO through momentum deposition of GWs propagating in the north/south direction. The resulting momentum source represents a third (generally odd) order non-linear function of the meridional winds, and this enables the oscillation, as in the case of the QBO for the zonal winds. Since the meridional winds are relatively small compared to the zonal winds, however, the vertical wavelength that maintains the MWO is much smaller, i.e., only about 10 km instead of 40 km for the QBO. Consistent with the associated increase of the viscous stress, the period of the MWO is then short compared with that of the QBO, i.e., only about 2 to 4 months. Depending on the strength of the GW forcing, the computed amplitudes of the MWO are typically 4 m/s in the upper stratosphere and mesosphere, and the associated temperature amplitudes are between about 2 and 3 K. These amplitudes may be observable with the instruments on the TIMED spacecraft. Extended computer simulations with the NSM in 2D and 3D reveal that the MWO is modulated by and in turn influences the QBO.

I. Introduction

At low latitudes primarily, oscillations are observed in the zonal circulation, i.e., the quasi-biennial oscillation (QBO) with a period around 2 years and the semi-annual oscillation (SAO) with a period of 6 months that is tied to the seasonal variations in the solar heating. The QBO is observed in the stratosphere (Reed, 1965, and reviewed by Baldwin et al., 2000), has amplitudes close to 20 m/s and propagates down with a velocity of about 1.2 km/month. This oscillation has been observed also in the upper mesosphere (Burrage *et al.*, 1996). The SAO peaks in the stratosphere near 50 km with eastward and westward winds of about 20 m/s during equinox and solstice respectively. And a second peak with comparable magnitude but with opposite phase is observed in the upper mesosphere near 80 km (Hirota, 1980). Large variations by factors of 3-5 are observed in the SAO, which appear to be related to the QBO (Reddy and Vijayan, 1993; Garcia *et al.*, 1997; Dunkerton and Delisi, 1997).

Lindzen and Holton (1968) and Holton and Lindzen (1972) explained the QBO by invoking critical level absorption and radiative damping of equatorial planetary waves, the eastward propagating Kelvin waves and the westward propagating mixed Rossby-gravity (RG) waves. Their theory was elucidated by Plumb (1977) and Plumb and Bell (1982) and others (Baldwin et al., 2000), and Dunkerton (1979) extended it to explain also the SAO in the stratosphere. Satellite measurements (e.g., Hitchman and Leovy, 1988) and model results (e.g., Hamilton *et al.*, 1995) have shown more recently that the observed amplitudes of the equatorial planetary waves, the Kelvin waves, RG waves, and Rossby waves, are not large enough to reproduce the observed SAO; and the QBO also could not be generated (e.g., Takahashi and Boville, 1992; Hamilton *et al.*, 1995). Internal gravity waves, parameterized first by Lindzen (1981), have therefore been invoked as a possible additional source to drive the SAO and QBO in the stratosphere (see the reviews of Dunkerton, 1997; Dunkerton and Delisi, 1997, Baldwin et al.,

2000). Dunkerton (1982) had earlier invoked such waves to explain the observed SAO in the upper mesosphere.

Takahashi (1999) recently simulated the QBO with a GCM that had sufficient horizontal resolution to describe GWs. But to account for these wave interactions in a global-scale model generally requires parameterization. Lindzen (1981) was he first to develop such a scheme, and Dunkerton (1982b, c), Fritts and Lu (1993) and others followed. Complementing the effects of planetary waves, Dunkerton (1997) employed such a GW parameterization to successfully simulate the QBO in the stratosphere. In our modeling studies, we have employed the Doppler Spread Parameterization (DSP) of Hines (1997a, b). We have incorporated the DSP into the Numerical Spectral Model (NSM), introduced by Chan *et al.* (1994), to describe the temperature and wind fields of the stratosphere and mesosphere (Mengel *et al.*, 1995; Mayr *et al.*, 1997, 1998a). The GW momentum source in the NSM produces SAO and QBO amplitudes extending from the stratosphere into the upper mesosphere, which are comparable to those observed.

In the Earth's atmosphere, convection and winds over rough terrain generate gravity waves, which to first order are generated isotropically so that they propagate horizontally into all directions, to the east, west north, and south. As these waves propagate up and increase in amplitude due to the decreasing atmospheric density, they interact with the background flow to deposit momentum. The dynamical conditions dictate that the vertical and meridional winds are comparatively small so that the wave driven flow is mainly in the east-west direction. Thus, the QBO and SAO are generated primarily by GWs propagating in the east/west direction, much like eastward propagating Kelvin waves and westward propagating RG waves originally invoked to explain these oscillations.

The purpose of this paper is to discuss the effects of GWs propagating in the north/south direction, how these waves can affect the zonally symmetric (m = 0) meridional circulation. In section II, we shall briefly describe the model, which has been extensively discussed in the literature. In Section III, we shall present a study with the 2D version of the NSM, where we delineate the differences between numerical results obtained with and without the meridional momentum source. To complement Section III and provide some understanding, we shall present in Section IV results obtained with only the meridional momentum source. In this case, as expected, the equatorial oscillations in the zonal circulation do not develop, but a distinct short-period meridional wind oscillation is generated that appears to be the meridional counterpart to the QBO in the zonal circulation. In Section V, we present some results from the 3D version of the NSM, which also reveal a short-term meridional oscillation. We shall interpret the results in Section VI with the help a heuristic analytical formulation and summarize our conclusions in Section VII.

II. Model

The NSM we employ for studying the middle atmosphere is a global model extending from the Earth' surface into the thermosphere. The model is time dependent and fully nonlinear. It is simplified in that perturbation theory is applied to compute the wind fields and the temperature and density perturbations of an adopted globally-averaged background atmosphere. The model is driven by the solar radiation that provides the heat source and by a constant GW flux (originating near the ground in the troposphere) that provides a horizontal momentum source. The zonally averaged component (zonal wavenumber m = 0) of solar heating is due to UV radiation absorbed in the

stratosphere and mesosphere (Strobel, 1978) and by EUV radiation absorbed in the thermosphere. Tropospheric heating is not accounted for. In the 3D version of the NSM, the heating rates for the excitation of tides are due to Forbes and Garrett (1978). With the relative temperature perturbations being less than 10%, the radiative energy loss is formulated in terms of Newtonian cooling, which is provided by Zhu (1989). The vertical integration step for the NSM is typically about 0.5 km, and the maximum meridional wave number is $l = 12$ (12 Gaussian points per hemisphere to evaluate the non-linearities in physical space). Depending on the chosen model parameters, the time integration step is chosen between 5 and 15 minutes.

To describe the effects of GWs, the NSM incorporates Hines' Doppler Spread Parameterization (DSP), which deals with a spectrum of waves and quantifies how the waves drive and dampen the background wind field through which they propagate. The DSP also accounts for non-linear interactions between the waves, which in turn affects the wave mean flow interactions. As the waves in the spectrum propagate up, their amplitudes increase due to the decreasing density, and the advective non-linearity becomes increasingly more important with increasing vertical wavenumber. "Doppler Spreading" due to wave-wave interaction and Doppler shifting by the background winds cause the largest vertical wave numbers to be preferentially absorbed so that GW momentum (and energy) are deposited in the wind field of the background atmosphere.

In our modeling study, the assumptions for the DSP are kept deliberately simple. The GWs are assumed to originate near the ground level carrying the same momentum in the four compass directions. Their horizontally isotropic momentum flux may vary with latitude, but it does not vary with season so that the GWs do not force a particular periodicity on the flow.

Associated with deposition of momentum in the background atmosphere, the waves also deposit energy (ignored in the NSM) and enhance the diffusivity. The vertical eddy diffusion rate, K, thus generated, increases exponentially with height, roughly like $\rho^{-1/2}$, where ρ is the ambient mass density. This increase of K, in conformity with the growth of the GW momentum source (per mass), is important in generating the flow oscillations in the model.

Hines' DSP comes with parameterization factors of order one, which are uncertain and might vary by as much as a factor of four. In the NSM, the parameters for the GW momentum source are chosen simply from the middle of the recommended range. The DSP also employs parameterization factors that determine the eddy diffusivity, K, and characterize the source spectrum. While the model can be made to reproduce the essential features of the QBO (and other properties of the Earth's middle atmosphere such as tides), the numerical solutions are not unique, to a large extent because of uncertainties in the treatment of GWs for which the observations are still very limited.

III. Zonally Symmetric Oscillations with Zonal and Meridional GW Sources

For the study presented here, we carry out two numerical experiments with the 2D version of the NSM for which identical GW parameters are adopted. The experiments differ in that (1) both the zonal and meridional GW momentum sources are employed and for comparison (2) only the zonal (but not meridional) momentum source is accounted for. In each case, the model results produce the essential features that characterize the middle atmosphere, the QBO and SAO at low latitudes, and the global-scale annual variations exemplified by the temperature reversal in the upper mesosphere with lower and higher temperatures in the summer and winter hemispheres

respectively. For the same GW parameters, the numerical experiment presented in the subsequent section will then describe a solution obtained only with the meridional (but not zonal) GW momentum source. This experiment is mainly academic the results, for it does not reproduce the above dynamical features, but it does highlight the process that can generate the interseasonal variations discussed in this paper.

The GW parameters chosen for the numerical experiments are the following. The horizontal wind variability, σ_h, is chosen so that its value at 20 km is 3 m/s, which is typically observed at low latitude (Allen and Vincent, 1996). For the characteristic horizontal wavelength, k_*, we chose $(75\ km)^{-1}$, which is near the lower limit recommended by Hines' DSP. The GWs are released in the troposphere at 1 km altitude and are assumed to be generated isotropically and independent of latitude and season. The adopted eddy diffusion rate, related to the GW momentum deposition, increases with altitude but is taken to be independent of latitude and seasonal, and it is the same for the three numerical experiments.

With Figure 1, we present the computed meridional winds for a latitude of 4° at 20, 50 and 80 km altitudes obtained with zonal and meridional GW momentum sources (a) and for comparison computed only with the zonal component of the GW source (b). Since the meridional winds rapidly increase with height, different scales are adopted for different altitudes. At the beginning of a model year, at winter solstice, the Sun is in the southern hemisphere, and the wind direction is positive northward. In both cases and at 80 km, the meridional winds are large and they are dominated by the annual cycle, directed from the summer to the winter hemisphere. This is the meridional circulation that produces the seasonal temperature reversal in the upper mesosphere. With the meridional GW source included, the amplitudes are larger and much more variable on time scales of months. At 20 and 50 km, in contrast, the patterns that appear in the computed meridional winds are much less regular. At these altitudes, dynamical interactions are much less important compared with radiative forcing. Nevertheless, our model results show that the meridional momentum source can generate here wind velocities that are typically 3 m/s at 50 km and more than 1 m/s at 20 km, much larger than those produced when this momentum source is artificially suppressed (b). The results also indicate that, intermittently, the wind perturbations are amplified and modulated. This is evident in particular at 20 km where in intervals of more than 2.5 years the amplitudes are greatly enhanced.

The results presented with Figure 2 suggest that the QBO in part is the cause for the above discussed variability. Here we show as contour plots the zonal winds (a) and the meridional winds (b) computed with both components of the GW momentum source. The QBO in this case has a period of more than 30 months, near the upper end of the observed range. And this periodicity is also apparent in the meridional wind field, in particular at 30 km.

What causes the interseasonal variations that are produced by the meridional momentum source? To address this question, we show in Figure 3 snapshots of the height variations in the zonal and meridional winds and their related momentum sources, all taken at one particular time (model year 8, solstice). Since the relative variations are only of interest, the winds and momentum sources are normalized for convenience so that the variations can be resolved throughout the middle atmosphere. For the zonal winds, the normalization factor is height independent. But for the meridional winds that increase rapidly with height, the factor decreases with altitude. For the zonal momentum source the normalization factor is taken to increase with height at a rate proportional to $(\rho K)^{-1}$, which represents the effective wave induced acceleration. For the meridional momentum source, the normalization factor is chosen to be height independent.

In the case of the larger zonal winds (Figure 3a), where the vertical wavelength of the oscillation is large (more than 40 km), the related momentum source is narrow and is confined to the regions with the largest vertical velocity gradients. This is the signature property of the GW momentum deposition formulated with the DSP and discussed in detail by Mayr et al. (1998a, b), which results from GWs propagating eastward and westward with vertical wavenumbers mE and mW (shown normalized in Figure 3b). The eastward propagating waves that encounter a vertical gradient between 20 and 30 km in this case deposit momentum in relation to that gradient. As a result, the waves lose momentum as mE rapidly decreases with height, which tends to decrease exponentially on its own due to the decreasing ambient atmospheric density. At the same time, the westward propagating waves encounter eastward winds in the opposite direction, and this would cause mW to go negative. Since the latter is not allowed, mW is constraint by the DSP to remain constant with height. The DSP also imposes the constraint that mE or mW cannot increase with height, which would imply that GWs are resurrected. The formulation of the DSP, briefly alluded to here, thus produces a pattern of wave momentum deposition that facilitates the QBO and SAO to be generated in our model. An essential property of this momentum deposition is that it is a non-linear function of the wind field, and that the non-linearity is evidently of third (generally odd) order. For a given fundamental periodicity of the oscillation (around 2 years for the QBO), a non-linearity of this kind produces the corresponding higher harmonics. But it also produces the fundamental harmonic itself and thus maintains the oscillation – the fluid dynamical analog of the mechanical clock in which the escapement mechanism produces the impulse that keeps it going against the tendency of friction to bring the pendulum to a halt.

The situation for the meridional winds shown on the right hand side of Figure 3 appears to be similar to that for the zonal winds, in principle at least. Sharp peaks in the momentum deposition (Figure 3c) are located where the meridional winds, either northward or southward, increase with height. And these spikes in the momentum source are associated with step-like patters in the wavenumbers (Figure 3d), which resemble those shown in Figure 3b. The difference between the zonal and meridional components however is that the vertical wavelengths greatly differ, generally less than 10 km for the meridional wind perturbation and more than 40 km for the zonal winds. Since the meridional winds are small compared with the zonal winds, larger vertical gradients or smaller vertical wavelength are required to dissipate the GW momentum – and related to that the period of the perturbation is smaller to produce the interseasonal variations in the model. We shall discuss this trend in greater detail in subsequent sections.

Anticipating results later discussed, we may assume that the meridional wind perturbations are largely confined to low latitudes. The computed perturbations in the meridional wind field, shown in Figures 1 and 2, transport energy across the equator, which in turn tends to produce adiabatic heating and cooling in the opposite hemispheres. This being true, one should then expect that these wind perturbations produce temperature perturbations in both hemispheres, in addition to those driven by radiative heating and cooling. Figure 4 suggests that this indeed is happening. Here we present the temperature perturbations at 18° latitude computed (a) with both GW momentum sources and (b) with the zonal source only. As is the case for the meridional winds, the differences are large. At 80 km in particular, with only the zonal GW source turned on (b), the temperature variations are dominated by the annual cycle with larger temperatures in winter than in summer. In contrast to that, the interseasonal variations (with periods around 3 months) completely dominate at this altitude when the meridional momentum source is also applied. At 50 km, the differences are also large and are presumably induced to a large extent by

dynamics. But at 20 km, the effect of the meridional circulation is small. In both cases, with and without the meridional wave source, the temperature perturbations at this altitude are apparently dominated by the seasonal cycle related to radiative heating and cooling. Another way to present the computed temperature perturbations is shown with contour plots in Figure 5, where we concentrate on the altitude range between 50 and 90 km. Without the meridional wave source (b), the annual cycle tends to dominate, although not exclusively. When the meridional source is included (a), the interseasonal variations are more pronounced and not only at 80 km but at lower altitudes as well.

IV. GW Driven Meridional Oscillation

To shed further light on the GW driven perturbations of the meridional winds discussed in the previous section, we show here results from a numerical experiment in which the meridional momentum source was retained but the zonal momentum source was turned off. An experiment like this is only of academic interest for it cannot reproduce the essential dynamical features that characterize the middle atmosphere. It does not produce a QBO or a large enough SAO, and the seasonal temperature reversal in the upper mesosphere does not develop. But we believe that the results are of interest, for they highlight the basic process for generating meridional wind oscillations, which appears to be similar to the process that generates the zonal wind oscillations discussed originally by Lindzen and Holton.

In Figure 6, we show for a period of 2 years the resulting meridional wind oscillations over an altitude range between 20 and 80 km (with contour intervals of 1 m/s). A pronounced and fairly steady oscillation is seen here with a period of about 2 months that propagates down with a velocity that increases from about 2.5 km/month at lower attitudes to 5 km/month at 70 km. Except for the period and propagation velocity, and magnitude of the winds, the character of this oscillation resembles that of the QBO in the zonal winds.

That we are dealing here indeed with a distinct oscillation, is further underscored with Figure 7. This shows, analogous to Figure 3, snapshots of the wavenumbers (a), meridional winds and related momentum source (b), and snapshots of the winds at intervals of 4 weeks (c) to illustrate the downward propagation. The intermittent momentum deposition of GWs propagating in the north/south directions, shown in the staircase pattern of the vertical wavenumbers (a) produce spikes in the momentum deposition (b), whose nonlinearity enables the oscillation and concomitant downward propagation of the meridional wind pattern.

The above discussed meridional wind oscillation is largely confined to low latitudes as shown in Figure 8 with a contour plot in time and latitude at an altitude near 60 km. This reveals again a fairly regular pattern of short term oscillations, which are modulated by the annual cycle that is hemispherically asymmetric to reflect the position of the Sun. We surmise that the annual cycle in the meridional circulation, with winds blowing from the summer to the winter hemisphere, may stimulate the short term wind oscillations that are generated in this case.

The temperature variations from this numerical experiment with the meridional GW momentum source are presented in Figure 9. In the top panel (a) is a contour plot versus time and altitude at 4° latitude, which shows a distinct semiannual variation at around 45 km that is presumably due to radiative heating from the Sun crossing the equator twice a year during spring and fall. At altitudes above 55 km, distinct interseasonal variations appear that are apparently related to the above discussed meridional wind oscillations. Away from the equator at 18°

latitude (b), these oscillations completely dominate throughout the middle atmosphere, presumably because of the adiabatic heating and cooling that is produced by meridional wind oscillations such as shown in Figure 8. At higher latitudes (c), the seasonal cycle from the Sun's radiative heating dominates, with lower and higher temperatures in winter and summer respectively. As pointed out earlier, the observed seasonal temperature reversal above 70 km cannot be reproduced in this case where the zonal GW momentum source is artificially suppressed.

From the above discussed numerical experiment that accounts only for the meridional GW source we learn that a distinct and persistent meridional wind oscillation can be generated. Although this situation does not resemble reality for all the reasons mentioned, it does provide some understanding of the interseasonal variations, which were earlier discussed with a model that accounts also for the zonal GW momentum source. In that more realistic case, the wave driven QBO and SAO are apparently generating zonal wind oscillations, which greatly influence and tear up the meridional wind oscillations to produce a complicated picture of interseasonal variations. That this is likely true is apparent from the modulation of the meridional wind oscillations by the QBO as seen from Figure 2.

V. 3D Model Result

We have also began carrying out experiments with the 3D version of our NSM, and some preliminary results are shown here to demonstrate that meridional oscillations are also being generated there. The GW parameters chosen in this case are different, in part because GW momentum is expended not only to influence the axisymmetric (m = 0) circulation but it affects also the tides and planetary waves in the middle atmosphere (Mayr et al., 2001a, b). For the model result presented, the GWs are again assumed to be generated isotropically and independent of season, but the GW induced horizontal wind variability, σ_h, is chosen to peak at the equator in better agreement with observations (Allen and Vincent, 1995). Specifically, the GW parameters are taken to be $k_* = (100\ km)^{-1}$ and $\sigma_h(20\ km) = 3$ m/s (equator), $\sigma_h(20\ km) = 2$ m/s at mid latitudes. The GW source is assumed to be located at an altitude of 3 km.

Analogous to Figure 1 from the 2D model, we present here with Figure 10 at 4° latitude the meridional winds for the zonally symmetric component (m = 0) computed with the meridional and zonal GW momentum sources (a) and for comparison with the zonal source only (b). This shows again, in both cases, relatively large meridional winds at 80 km, which blow from the summer to the winter hemisphere. As discussed earlier, these winds are driven primarily by the zonal component of the GW source (Lindzen, 1980), but they are modulated also by the meridional component of the wave source. At 50 km altitude, the interseasonal variations are much larger with the meridional source included, and at 20 km this source solely accounts for the meridional winds that are generated there. The modulations seen in the meridional winds, both at 50 and 20 km, indicate that the QBO is effective. This is confirmed with Figure 11, where we present for 4° latitude the zonal (a) and meridional (b) wind velocities. In this case, the QBO has a period of about 24 months. As in Figure 2, the meridional GW source generates meridional wind perturbations that in turn are modulated by the QBO.

Our results reveal that the meridional wind perturbations computed in the model are well organized as shown in Figure 12 with 7-day resolution for time spans of 2 model years. The patterns seen here are recurring with remarkable persistency in about 2-year intervals throughout

the 20-year model run, which indicates that we are dealing with a robust dynamical feature albeit one that is probably not unique but is determined by the adopted specific GW forcing.

As is the case for the 2D model, the meridional wind perturbations in 3D are also confined largely to low latitudes, and this is shown with Figure 13. This again suggests that the interhemispheric, solar driven meridional circulation is playing an important role to stimulate these wind perturbations and modulate them like a pacemaker.

VI. Discussion

In modeling the dynamics of the middle atmosphere, there is now compelling evidence that small scale gravity waves are playing an important role. This is true not only for the upper mesosphere, where these waves have been invoked to explain to a large extent the observed anomalous seasonal variations in the temperature and zonal circulation (Lindzen, 1981). Gravity waves are now believed to be also important at lower altitudes for generating the observed QBO and SAO near the equator (e.g., Dunkerton, 1997). Short of simulating these waves from first principle with a GCM, which has been accomplished (Takahashi, 2000) but still remains difficult with present computers, parameterization is required to incorporate their effects in global-scale models. The Doppler Spread Parameterization developed by Hines (1997a, b) allows us to describe the major dynamical features that characterize the middle atmosphere, including the QBO and SAO extending from the stratosphere into the upper mesosphere, the seasonal variations of tides, and the generation of planetary waves.

Our experience shows that the uncertainties in the GW parameterization and the lack of observations to tie it down, combined with the uncertainties in the eddy diffusivities, all make it virtually impossible to design a model that is reasonably unique. For example, the period and magnitude of the QBO can be changed by adopting a different rate of eddy diffusion and by changing the height where the GWs are generated.

At this early stage of exploring the effects of GWs, we therefore believe that numerical experiments remain useful to explore the physical properties of the dynamical system. To that end, we have explored here the dynamical process, earlier ignored, in which GWs deposit momentum in the zonally symmetric meridional circulation to produce interseasonal variations. Our approach has been to design numerical experiments that are deliberately simple so that some basic understanding can be gained. The idea is that, as our understanding gradually evolves, an increasingly more realistic model can be developed to simulate the observations in greater detail.

The process we have been describing here is due to GWs that propagate in the north/south directions to accelerate the meridional circulation. The meridional winds of the zonally symmetric ($m = 0$) component are generally very small compared to the zonal winds that tend to be produced either by geostrophic balance or by the interaction of east/west propagating waves at low latitudes (i.e., the QBO and SAO). Unlike the axisymmetric zonal winds that are solenoidal and therefore are not involved directly in redistributing energy, the meridional winds have divergence to produce adiabatic heating and cooling, and this greatly dampens the motions.

In order for the GWs to generate an oscillation in the small meridional winds, it helps that the vertical wavelength of the flow perturbation is also small. The small vertical wavelength in turn helps to produce the non-linear condition that maintains the oscillation. At the same time, the smaller vertical wavelength causes more viscous dissipation, which contributes to dampen the meridional winds.

It is here instructive to go into some of the details of the basic process, essentially nonlinear, in which GWs function to produce a wind oscillation. For this purpose we employ the simplified analytical formulation of the GW momentum source from the DSP (Mayr et al., 1998b), which serves us to provide an heuristic scale analysis. Assuming for the wind velocity $U = U_o e^{(ikz+i\omega t)}$, we obtain with this formulation a relationship for the momentum balance

$$i\omega\rho U + k^2 K\rho U + \gamma\rho U = \left[\frac{\rho_o \Phi^2 \sigma_h{}^4 k_*}{2N(\Phi\sigma_h + |U|)^2}\right]\left(ikU + \frac{\Phi\sigma_h}{3H|U|}U\right) \qquad (1)$$

where the left hand side, applied to the equator, describes the fluid dynamical forces due to inertia, viscous dissipation and horizontal pressure gradient, and the right hand side represents the GW momentum source. With the term, $\gamma\rho U$, we represent heuristically the damping of the meridional winds associated with adiabatic heating and cooling, which involves also the energy balance. Here, ρ_o is the density at the height where the wave source originates, and k and ω are respectively the vertical wavenumber and frequency of the flow oscillation. The GW parameter, Φ, is of order one, H is the density scale height, $\sigma_h \propto \approx \rho^{-1/3}$ is the GW horizontal wind variability, k_*, is the characteristic horizontal wave number for GWs, and N is the buoyancy frequency. As pointed out earlier, the momentum source on the right hand side of Eq. (1) represents a nonlinear function of the wind field, U, which is of third (odd) order such that it maintains the oscillation. With that non-linearity, one can then imagine that the solution for such an equation would determine the vertical wavelength of the wind oscillation in relation to (or depending upon) the magnitudes of the wind velocities.

For a qualitative trend analysis, we delineate the real and imaginary components

$$Kk^2 + \gamma \approx \frac{1}{\rho}\left[\frac{\rho_o \Phi^2 \sigma_h{}^4 k_*}{2N(\Phi\sigma_h + |U|)^2}\right]\frac{\Phi\sigma_h}{3H|U|} \qquad (2)$$

$$\omega \equiv \frac{2\pi}{\tau} \approx \frac{1}{\rho}\left[\frac{\rho_o \Phi^2 \sigma_h{}^4 k_*}{2N(\Phi\sigma_h + |U|)^2}\right]k \qquad (3)$$

where we taken |U| to be also the amplitude of $U(\omega, z)$. Without the pressure term on the left hand side, Eq. (2) applies to the zonal winds, $U = U_z$ at the equator, and it may serve to qualitatively "evaluate" their velocities in the sprit of the "Prototype Model" of Lindzen and Holton (1968). Since U_z appears in the denominators on the right hand side of Eq. (2), its magnitude decreases as Kk^2 increases. One would certainly expect that an increase in K, with more dissipation, should produce a solution in which the winds are reduced. And at the same time one may argue that for a given K the reduction in U_z would be associated with an increase in k. In other words it is reasonable to expect that an increase in K would lead not only to a reduction in U_z, it would also produce an increase in k – and this we have seen from numerical experiments for the zonal wind oscillations (Mayr et al., 1998a, Figure 7). With reduced U_z and concomitant increase in k, the frequency of the oscillation would then increase, which can be inferred from Eq. (3) and is shown in the same Figure 7.

For the meridional winds, U_m, the dynamical situation is more complicated. The pressure term on the left hand side of Eq. (2) can only be evaluated in the framework of 2D or 3D models that describe the full set of conservation equations to account also for energy balance. Notwithstanding this difficulty, we apply Eq. (2) in the spirit of the above analytical argument. For a given K, k^2 on the left hand side of Eq. (2) would tend to increase as U_m on the right decreases – and this is what the numerical results show for the oscillations of the small meridional winds in comparison with those for the much larger zonal winds. With the resulting small vertical wavelength, λ, the viscous dissipation $\propto k^2K = (2\pi/\lambda)^2K$ becomes more important relative to the pressure term, γ, in Eq. (2). Given then that the meridional winds are small compared with the zonal winds, $U_m << U_z$, and that $k_m >> k_z$, Eq.(3) then tells us that $\omega_m(U_m, k_m) >> \omega_z(U_z, k_z)$, which is seen in the numerical results discussed earlier. This also can explain why in the stratosphere the downward propagation velocity, ω/k, is larger for the meridional oscillation, i.e. 2.4 km/month (see Figure 6), compared to 1.2 km/month for the QBO in the zonal circulation.

Based on the arguments presented here, which are supported by numerical results, we are led to conclude that wave-driven nonlinear oscillations in a fluid can produce, in principle, depending on the dynamical condition, virtually any intrinsic frequency. A mechanical clock, another nonlinear oscillator, is typically designed with the length of the pendulum for a period of 1 sec. With insufficient energy to drive this device, or too much friction, the 1-sec pendulum cannot be kept in motion. In contrast to that, a fluid has no such design. With the right kind of wave interaction, such as delivered by GWs as inferred from Hines' DSP, oscillations should develop in a fluid, in principle, no matter how small the forcing or how large the dissipation. Intuitively it seems reasonable that longer periods are associated with massive and energetic dynamical systems – the heart period and life span of the elephant being much longer than those of the fly.

VII. Conclusion

With our Numerical Spectral Model, having a vertical grid point resolution of about 0.5 km, we have shown that the momentum source from GWs propagating in the north/south direction can generate axisymmetric meridional wind oscillations (MWO) or perturbations that may contribute significantly to produce interseasonal variations in the middle atmosphere. Compared with the zonal winds, the meridional winds are being dampened by the pressure feedback due to adiabatic heating and cooling, and as a result the winds are relatively small. That being true, larger vertical velocity gradients are required to dissipate GW momentum and energy, so that the vertical wavelength of the meridional wind perturbation is much smaller than that of the zonal oscillation, i.e., the QBO and SAO. The comparatively small meridional velocities and related small vertical wavelength of oscillation translate into larger vertical propagation velocities of the perturbations and into smaller oscillation periods, between 1 and 4 months.

Based on a modeling study, we have provided here an initial report on a potentially interesting dynamical feature of the middle atmosphere that, to our knowledge, has not been discussed in the literature before. We have developed enough of an understanding to be confident that GWs with north/south component of propagation can generate meridional wind perturbations that have periods on the order of months. And associated with that, temperature perturbations develop. From our modeling study, we learn that these perturbations appear to be

modulated by the seasonal cycle and by the QBO, and we find that the underlying meridional GW momentum source also affects the equatorial zonal wind oscillations including the QBO.

A number of questions remain, and some of them are briefly addressed here:

1.) Foremost of all is the question whether there are observable signatures of the above discussed phenomenon, in the meridional winds, in the temperature perturbation, in ozone or other tracers of the meridional wind field. This is also a very difficult question, because a great number of other processes may produce similar signatures in the atmosphere especially in the framework of the 3D dynamics.

2.) Our numerical experiments show that the meridional GW momentum source can affect significantly the QBO and SAO in the zonal winds, though it cannot produce on its own any of the features that characterize these oscillations. The large-scale meridional circulation is involved in redistributing some of the zonal momentum in the QBO and SAO, and it is reasonable to expect that the meridional momentum deposited by GWs would affect this process. But the general properties of the effect still need to be explored.

3.) We believe to understand how the nonlinear nature of the GW forcing can produce oscillations in the small meridional winds with periods of only a few months as seen in our numerical results. But we do not understand how the seasonal variations and the QBO and SAO come into play to modulate these perturbations.

4.) The meridional wind perturbations generated by the GWs would in turn produce effective horizontal eddy diffusion, which should be evaluated.

Acknowledgement

One of us (HGM) is greatly indebted to Drs. E. Talaat, Johns Hopkins Applied Physics Laboratory and C. L. Wolff, Goddard Space Flight Center, for valuable discussions.

References

Allen, S.J., Vincent, R.A., 1995. Gravity wave activity in the lower atmosphere: Seasonal and latitudinal variations, J. Geophys. Res., 100, 1327.

Baldwin, M. P., Gray, L.J., Dunkerton, T.J., Hamilton, K., Haynes, P.H., Randel, W.J., Holton, J.R., Alexander, M.J., Hirota, I., Horinouchi, T., Jones, D.B.A., Kinnersley, J.S., Marquardt, C., Sato, K., Takahashi, M., 2001. The Quasi-Biennial Oscillation, Reviews of Geophysics, 39, 179.

Baldwin, M.P., Dunkerton, T.J., 1998. Biennial, quasi-biennial, and decadal oscillations of potential vorticity in the northern stratosphere, J. Geophys. Res., 103, 3919.

Burrage, M.D., Vincent, R.A, Mayr, H.G., Skinner, W.R., Arnold, N.F., Hays, P.B., 1996. Long-term variability in the equatorial middle atmosphere zonal wind, J. Geophys. Res., 101, 12847.

Chan, K.L., Mayr, H.G., Mengel, J.G., Harris, I.,1994. A 'stratified' spectral model for stable and convective atmospheres, J. Comput. Phys., 113, 165.

Dunkerton, T.J., 1979. On the role of the Kelvin wave in the westerly phase of the semiannual zonal wind oscillation, J. Atmos. Sci., 36, 32.

Dunkerton, T.J., 1982a. Theory of the mesopause semiannual oscillation, J. Atmos. Sci., 39, 2681.

Dunkerton, T.J., 1982b. Wave transcience in a compressible atmosphere. 3, The saturation of internal gravity waves in the mesosphere, J. Atmos. Sci., 39, 1042.

Dunkerton, T.J., 1982c. Stochastic parameterization of gravity wave stresses, J. Atmos. Sci., 39, 1711. Dunkerton, T.J., 1985. A two-dimensional model of the quasi-biennial oscillation, J. Atmos. Sci., 42, 1151.
Dunkerton, T.J., 1997. The role of gravity waves in the quasi-biennial oscillation, J. Geophys. Res., 102, 26053.
Dunkerton, T.J., Baldwin, M. P., 1992. Modes of interannual variability in the stratosphere, Geophys. Res. Lett., 19, 49.
Dunkerton, T.J., Delisi, D.P., 1997. Interaction of the quasi-biennial oscillation and the stratopause semiannual oscillation, J. Geophys. Res., 102, 26107.
Forbes, J.M, Garrett, HB, 1978. Thermal excitation of atmospheric tides due to insolation absorption by O_3 and H_2O. Geophys. Res. Lett., 5, 1013.
Fritts, D.C., Lu, W., 1993. Spectral estimates of gravity wave energy and momentum fluxes: II, Parameterization of wave forcing and variability, J. Atmos. Sci., 50, 3695.
Garcia, R.R., Dunkerton, T.J., Lieberman, R.S., Vincent, R.A., 1997. Climatology of the semiannual oscillation of the tropical middle atmosphere, J. Geophys. Res., 102, 26014.
Hamilton, K., Wilson, R.J., Mahlman, J.D., Umscheid, L.J., 1995. Climatology of the SKYHI troposphere-stratosphere-mesosphere general circulation model, J. Atmos. Sci., 52, 5.
Hamilton, K., 1986. Dynamics of the stratospheric semi-annual oscillation, J. Meteorol. Soc. Jpn., 64, 227.
Hines, C.O., 1997a. Doppler-spread parameterization of gravity-wave momentum deposition in the middle atmosphere, 1, Basic formulation, J. Atmos. Solar Terr. Phys., 59, 371.
Hines, C.O., 1997b. Doppler-spread parameterization of gravity-wave momentum deposition in the middle atmosphere, 2, Broad and quasi monochromatic spectra, and implementation, J. Atmos. Solar Terr. Phys., 59, 387.
Hirota, I., 1980. Observational evidence of the semiannual oscillation in the tropical middle atmosphere - a review, Pure Appl. Geophys., 118, 217.
Hitchman, M.H., Leovy, C.B., 1988. Estimation of the Kelvin wave contribution to the semiannual oscillation, J. Atmos. Sci., 45, 1462.
Holton, J.R., Lindzen, R.S., 1972. An updated theory for the quasi-biennial cycle of the tropical stratosphere, J Atmos. Sci., 29, 1076.
Holton, J.R., Tan, H.C., 1980. The influence of the equatorial quasi-biennial oscillation on the global circulation, at 50 mb, J. Atmos. Sci., 37, 2200.
Lindzen, R.S., Holton, J.R., 1968. A theory of the quasi-biennial oscillation, J. Atmos. Sci., 25, 1095.
Lindzen R.S., 1981. Turbulence and stress due to gravity wave and tidal breakdown, J. Geophys., Res., 86, 9707.
Mayr, H.G, Mengel, J.G., and Chan, K.L., 1998a. Equatorial oscillations maintained by gravity waves as described with the Doppler Spread Parameterization: I, Numerical experiments, J. Atmos. Solar Terr. Phys., 60, 181.
Mayr, H.G, Hartle, R.E., and Chan, K.L., 1998b. Equatorial oscillations maintained by gravity waves as described with the Doppler Spread Parameterization: II, Heuristic analysis, J. Atmos. Solar Terr. Phys., 60, 201.
Mayr, H.G, Mengel, J.G., Reddy, C.A., Chan, K.L., Porter, H.S., 1998. Variability of the equatorial oscillations induced by gravity wave filtering, Geophys. Res. Lett., 25 , 2629.

Mayr, H.G, Mengel, J.G., Hines, C.O., Chan, K.L., Arnold, N.F., Reddy, C.A., Porter, H.S., 1997. The gravity wave Doppler spread theory applied in a numerical spectral model of the middle atmosphere, 2, Equatorial oscillations, J. Geophys. Res., 102, 26093.

Mengel, J.G., Mayr, H.G., Chan, K.L., Hines, C.O., Reddy, C.A., Arnold, N.F., Porter, H.S., 1995. Equatorial oscillations in the middle atmosphere generated by small scale gravity waves, Geophys. Res. Lett., 22 , 3027.

Naito, Y., Hirota, I., 1997. Interannual variability of the northern winter stratospheric circulation related to the QBO and the solar cycle, J. Meteorol. Soc., Jpn., 75, 925.

Plumb, R.A., 1977. The interaction of two internal waves with the mean flow: Implications for the theory of the quasi-biennial oscillation, J. Atmos. Sci., 34, 1847.

Plumb, R.A., R.C. Bell, 1982. A model of the quasi-biennial oscillation on an equatorial beta-plane, Q. J. R. Meteorol. Soc., 108, 335.

Plumb, R.A., 1984. The quasi-biennial oscillation, in Dynamics of the Middle Atmosphere, edited by J. R. Holton and T. Matsuna, pp. 217, Terra Sci., Tokyo.

Reed, R.J., 1965. The quasi-biennial oscillation of the atmosphere between 30 and 50 km over Ascension Island, J. Atmos. Sci., 22, 331.

Reed, R.J., 1966. Zonal wind behavior in the equatorial stratosphere and lower mesosphere, J. Geophys. Res., 71, 4223.

Strobel, D.F., 1978. Parameterization of atmospheric heating rate from 15 to 120 km due to O2 and O3 absorption of solar radiation, J. Geophys. Res., 83, 7963.

Takahashi, M., 1999. Simulation of the quasi-biennial oscillation in a general circulation model, Geophys. Res. Lett., 26 , 1307.

Takahashi, M., Boville, B.A., 1992. A three-dimensional simulation of the equatorial quasi-biennial oscillation, J. Atmos., Sci., 49, 1020.

Zhu, X., 1989. Radiative cooling calculated by random band models with S-1-beta tailed distribution, J. Atmos., Sci., 46, 511.

Figure Captions

Figure 1. Computed time series of the axisymmetric component (zonal wavenumber m = 0) of the meridional wind at 4° latitude for 20, 50, 80 km altitudes, computed with (a) meridional and zonal GW momentum sources, and (b) with zonal source only. The model results are recorded in 7 day intervals, and the 14 day running mean is presented.

Figure 2. Contour plot in altitude and time of computed zonal (a) and meridional (b) winds at 4° latitude, computed with both GW momentum sources. The results are averaged over a period of 28 days. Note that the meridional winds are modulated by the QBO.

Figure 3. Snapshots of the zonal (a) and meridional (c) winds and their associated GW momentum sources. The non-linear nature of the GW interaction with the background winds causes sharp peaks in the momentum deposition, which is very pronounced for the zonal component (a), but it is also evident for the meridional component (b). This non-linearity is apparently of third (odd) order, which enables the oscillations, and it is produced with the characteristic staircase patterns in the vertical wavenumbers (m from the DSP) by GWs propagating to the east (mE) and west (mW) in (b), and by waves propagating to the north (mN)

and south (mS) in (d). Note that the vertical wavelength of the meridional flow perturbation (c) is typically much shorter than that of the zonal flow oscillation (b).

Figure 4. Time series of computed temperature perturbations similar to Figure 1 but at 18° latitude where the meridional wind perturbations become very effective. The variations are caused by radiative heating and cooling and by transport processes. With the meridional GW source included (a), the interseasonal variations are significantly larger at 50 and 80 km altitudes.

Figure 5. Contour plots of computed temperature perturbations at 18° latitude, complementing Figure 4.

Figure 6. Contour plot of meridional winds computed with only the meridional GW momentum source. The characteristic meridional circulation from the summer to the winter hemisphere, seen in Figure 1 at 80 km, is not produced in this case. And the associated seasonal temperature reversal in the upper mesosphere is not generated either. Also, there is no QBO produced, and the SAO is much weaker than observed. But this numerical experiment demonstrates that the meridional momentum source can generate short term oscillations in the zonally symmetric meridional circulation that are apparently at the core of the perturbations shown earlier. This kind of oscillation also propagates down, like the QBO, but the propagation velocity is larger and the period is much shorter.

Figure 7. Snapshots of the meridional wind oscillations (computed with only the meridional GW momentum source) and associated GW momentum source and vertical wavenumbers, similar to Figure 3. The snapshots in (c) are 28 days apart and indicate downward propagation.

Figure 8. Contour plot in time and latitude of meridional winds (computed with only the meridional GW momentum source) at an altitude near 60 km. Note that the wind oscillation tends to be confined to low latitudes, presumably because it is seeded by the interhemispheric meridional circulation.

Figure 9. Temperature perturbations (computed with only the meridional GW momentum source) at 4, 18 and 33 degrees latitude. Near the equator, the semiannual variation dominates below 50 km due to radiative heating from the Sun. At 33° latitude, and higher, the annual variation dominates, with larger temperatures in Summer than in Winter. But at 18° latitude (and at 4° above 50 km), the interseasonal variations dominate that are driven by the meridional wind oscillation.

Figure 10. Meridional winds at 4° latitude, similar to Figure 1, but computed with the 3D model. In this case, the winds are presented at 7 day intervals at the rate the results are recorded. Note again that the winds at 80 km are driven primarily by the zonal GW momentum source, though there is more variability when the meridional source is included (a). At 20 and 50 km, the variations are much larger with that source, and they reveal a persistent pattern of modulation.

Figure 11. Zonal and meridional winds at 4° latitude, similar to Figure 2, but computed with the 3D model. The QBO in this case has a period close to 24 months, and it modulates the

meridional wind perturbations to produce a persistent and repeatable pattern, which is brought out in Figure 12.

Figure 12. Meridional winds at 4° latitude presented with a time resolution of 7 days. Over a period of several years, such pattern appears in the model with remarkable persistency to indicate that it is a robust feature of this particular model run.

Figure 13. Meridional winds at an altitude near 60 km computed with the 3D model and presented at 7 day intervals. As in Figure 8, the wind oscillations are mainly confined to low latitudes.

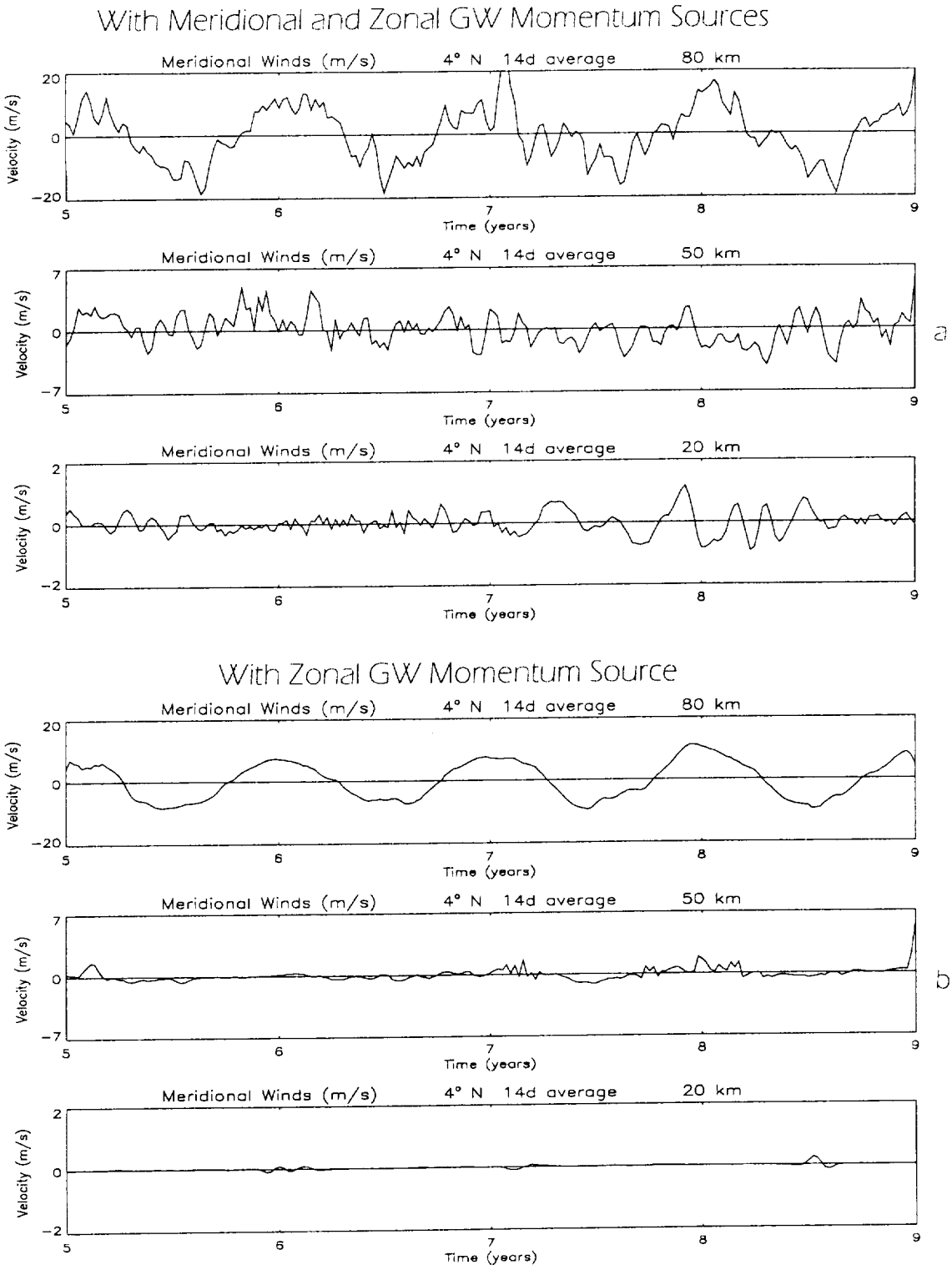
With Meridional and Zonal GW Momentum Sources
Meridional Winds (m/s) 4° N 14d average 80 km
Velocity (m/s)
Time (years)
Meridional Winds (m/s) 4° N 14d average 50 km
Velocity (m/s)
Time (years)
Meridional Winds (m/s) 4° N 14d average 20 km
Velocity (m/s)
Time (years)
a
With Zonal GW Momentum Source
Meridional Winds (m/s) 4° N 14d average 80 km
Velocity (m/s)
Time (years)
Meridional Winds (m/s) 4° N 14d average 50 km
Velocity (m/s)
Time (years)
Meridional Winds (m/s) 4° N 14d average 20 km
Velocity (m/s)
Time (years)
b

Figure 1

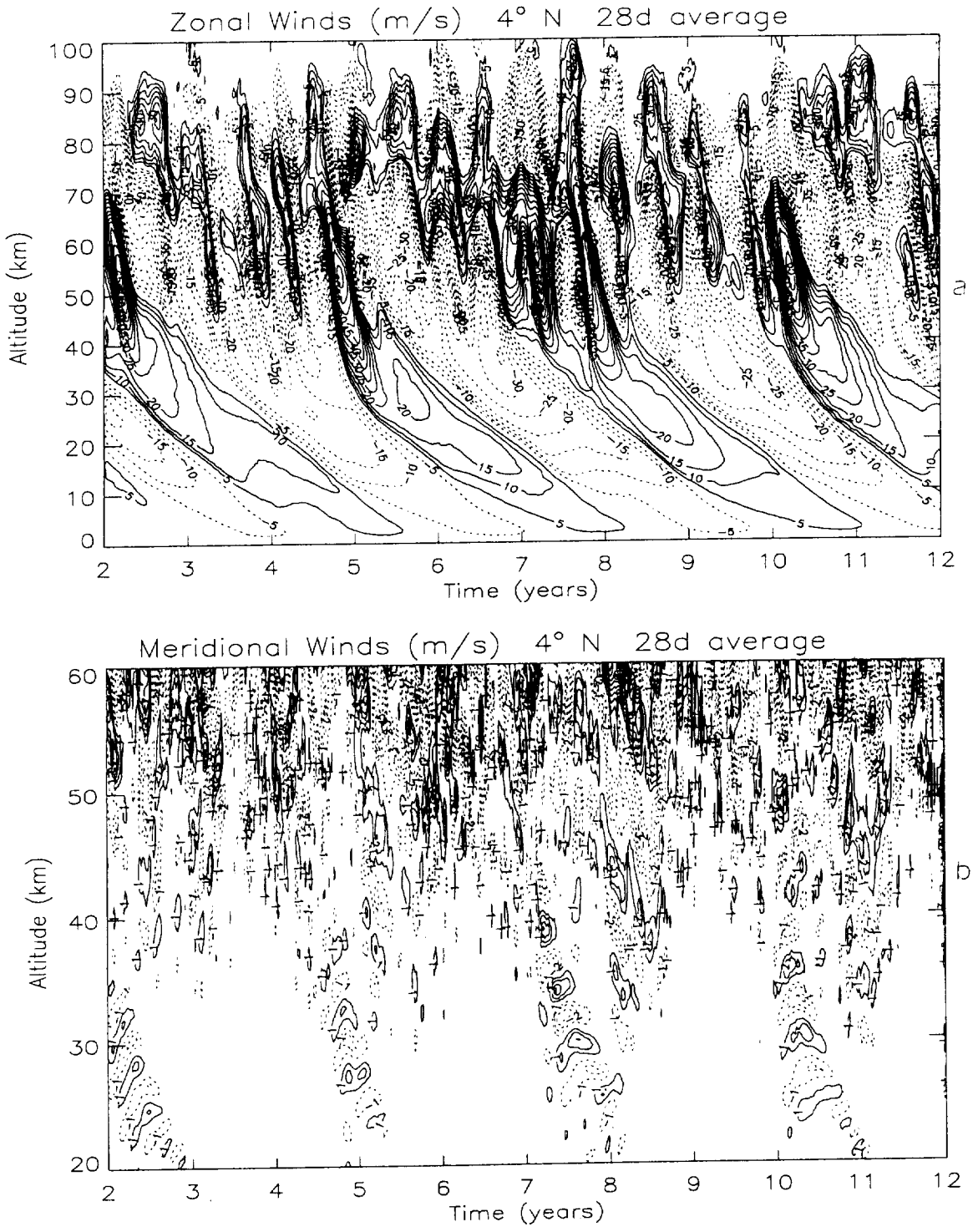
Zonal Winds (m/s) 4° N 28d average
Altitude (km)
Time (years)
a
Meridional Winds (m/s) 4° N 28d average
Altitude (km)
Time (years)
b

Figure 2

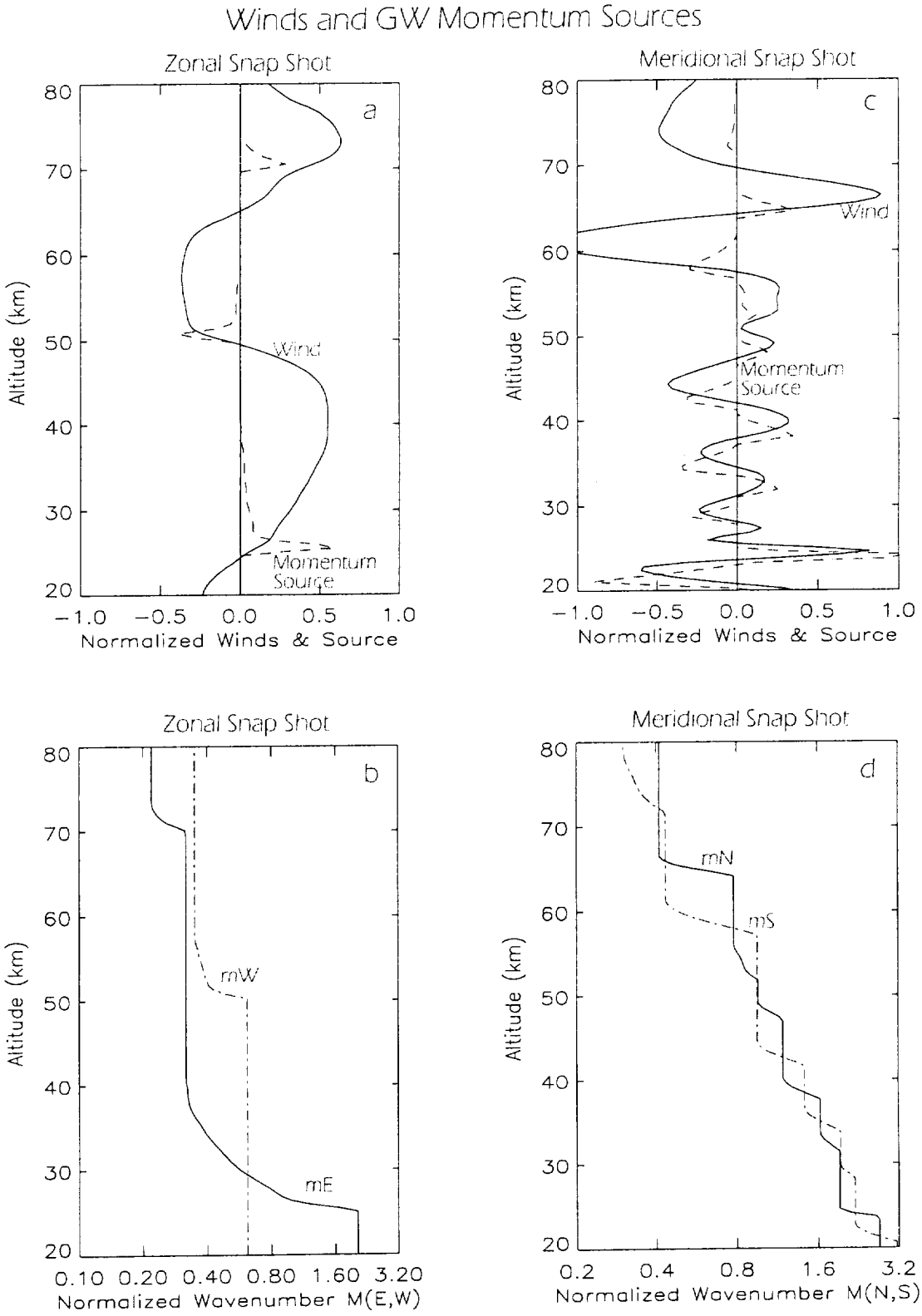
Winds and GW Momentum Sources
Zonal Snap Shot
a
Wind
Momentum Source
Altitude (km)
Normalized Winds & Source
Meridional Snap Shot
c
Wind
Momentum Source
Altitude (km)
Normalized Winds & Source
Zonal Snap Shot
b
mW
mE
Altitude (km)
Normalized Wavenumber M(E,W)
Meridional Snap Shot
d
mN
mS
Altitude (km)
Normalized Wavenumber M(N,S)

Figure 3

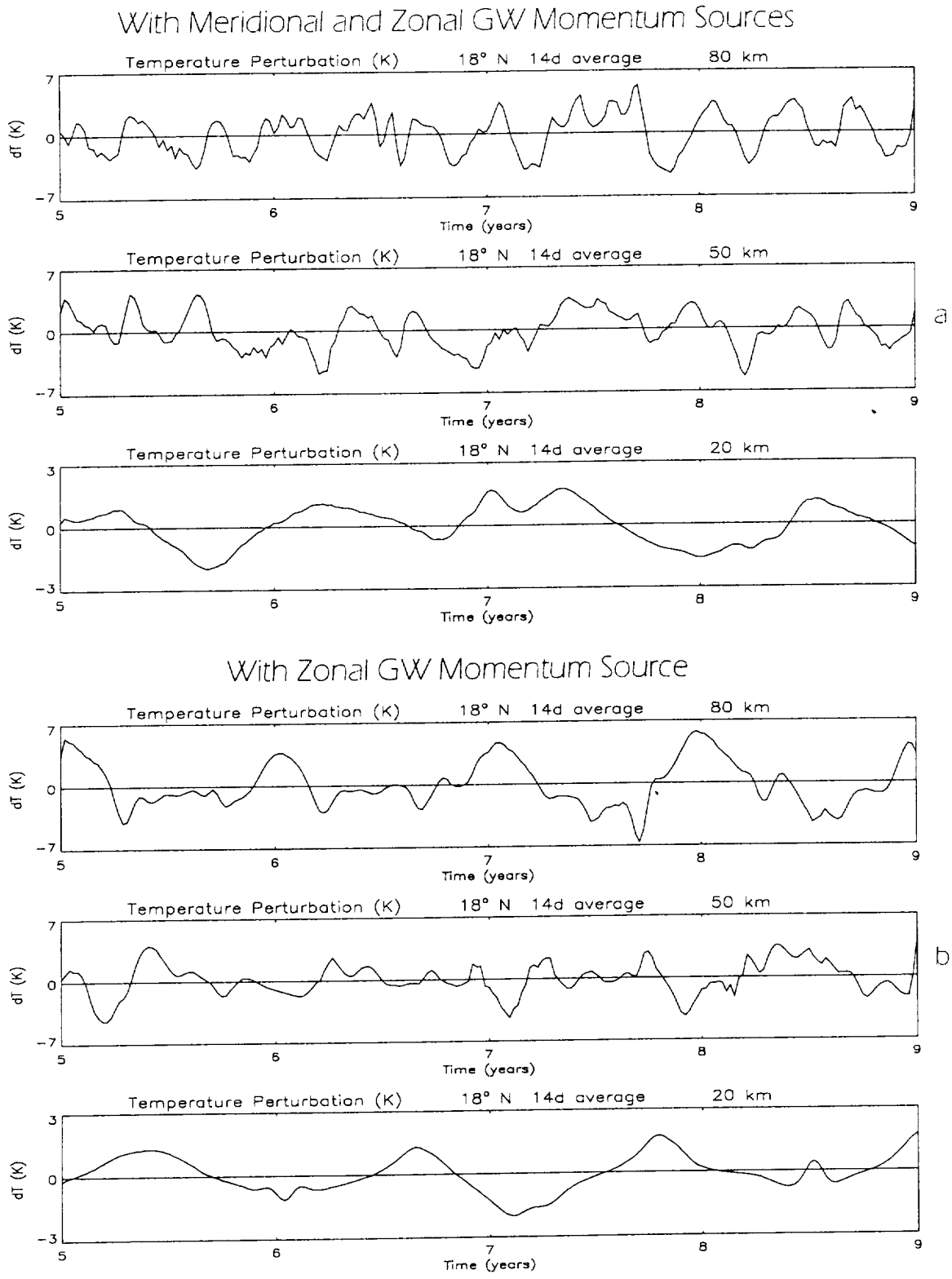
With Meridional and Zonal GW Momentum Sources
Temperature Perturbation (K) 18° N 14d average 80 km
dT (K)
Time (years)
Temperature Perturbation (K) 18° N 14d average 50 km
dT (K)
Time (years)
a
Temperature Perturbation (K) 18° N 14d average 20 km
dT (K)
Time (years)
With Zonal GW Momentum Source
Temperature Perturbation (K) 18° N 14d average 80 km
dT (K)
Time (years)
Temperature Perturbation (K) 18° N 14d average 50 km
dT (K)
Time (years)
b
Temperature Perturbation (K) 18° N 14d average 20 km
dT (K)
Time (years)

Figure 4.

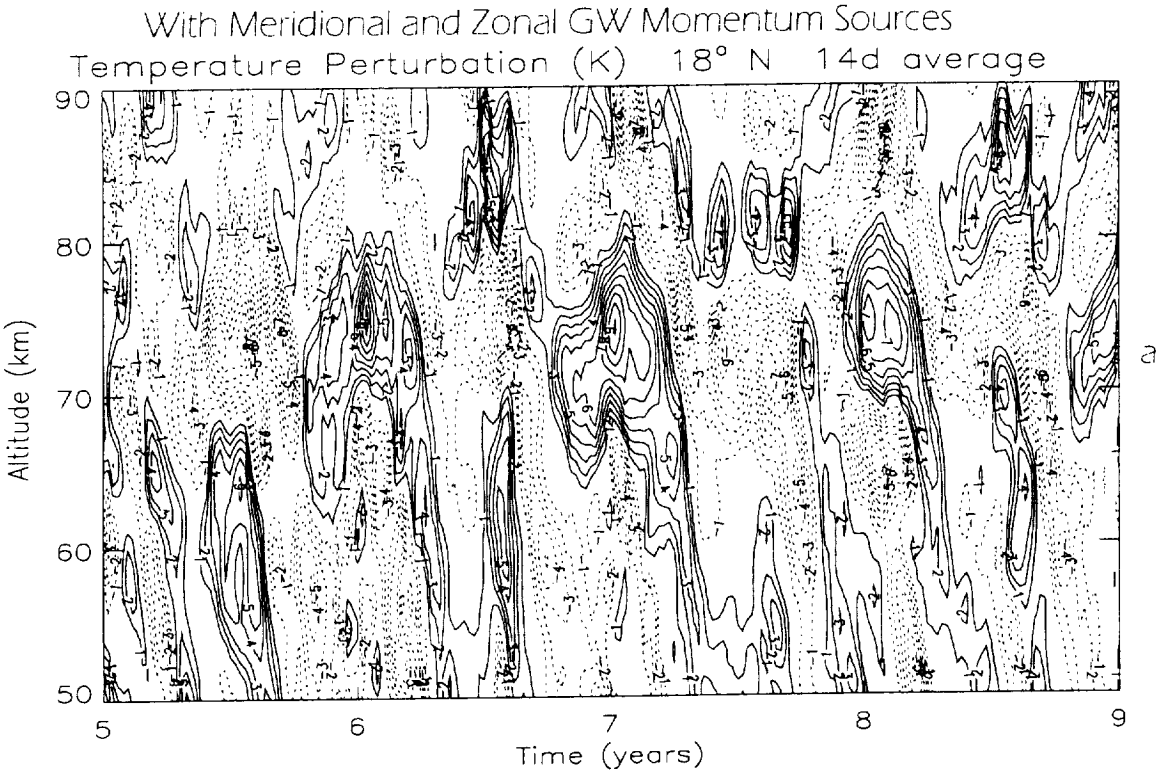
With Meridional and Zonal GW Momentum Sources
Temperature Perturbation (K) 18° N 14d average
Altitude (km)
90
80
70
60
50
5
6
7
8
9
Time (years)
a

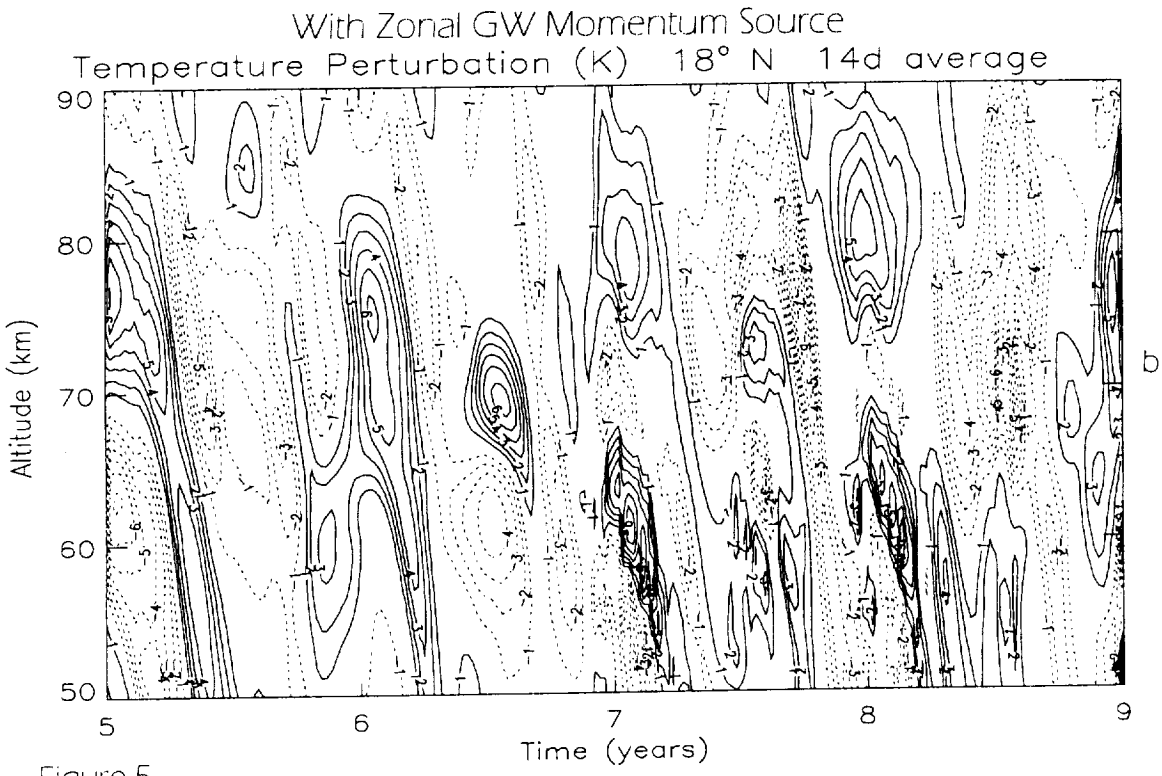
With Zonal GW Momentum Source
Temperature Perturbation (K) 18° N 14d average
Altitude (km)
90
80
70
60
50
5
6
7
8
9
Time (years)
b

Figure 5

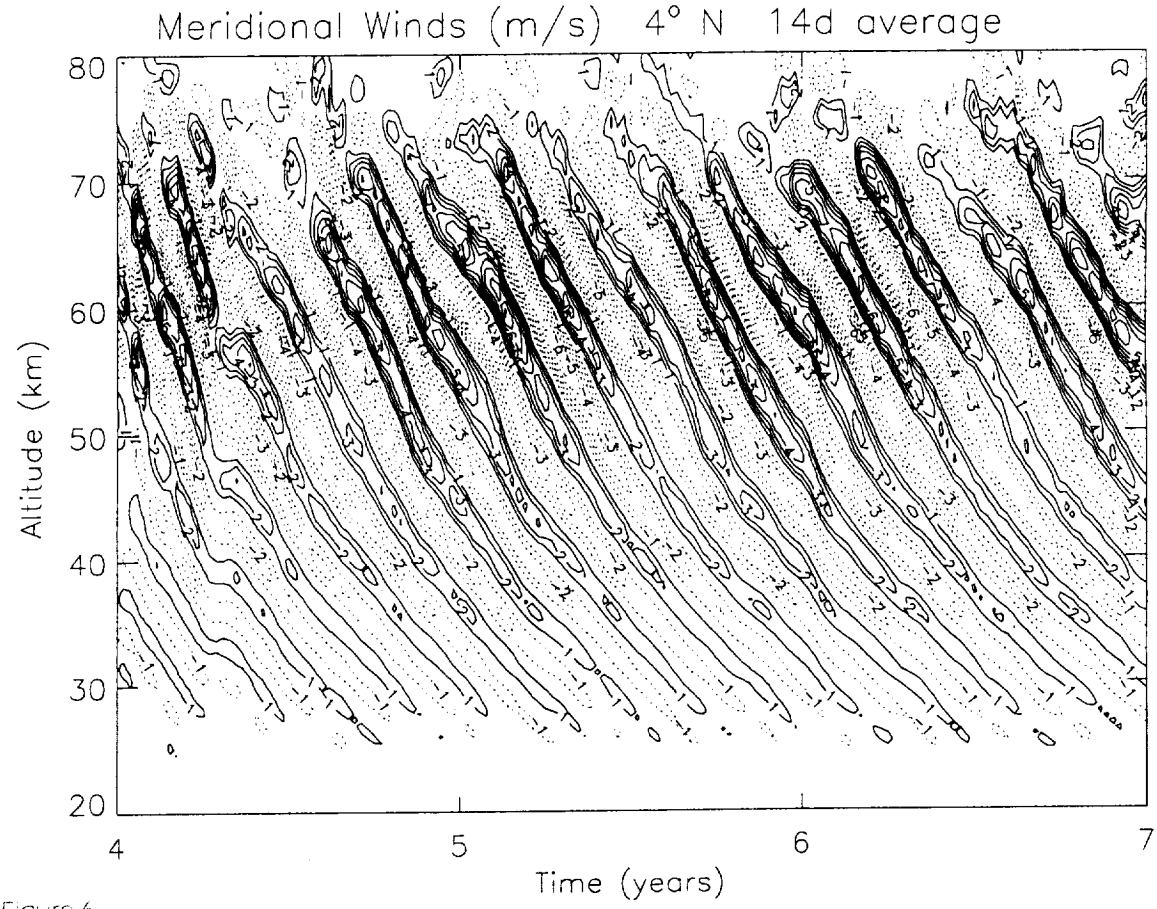
Meridional Winds (m/s) 4° N 14d average
Altitude (km)
80
70
60
50
40
30
20
4
5
6
7
Time (years)

Figure 6

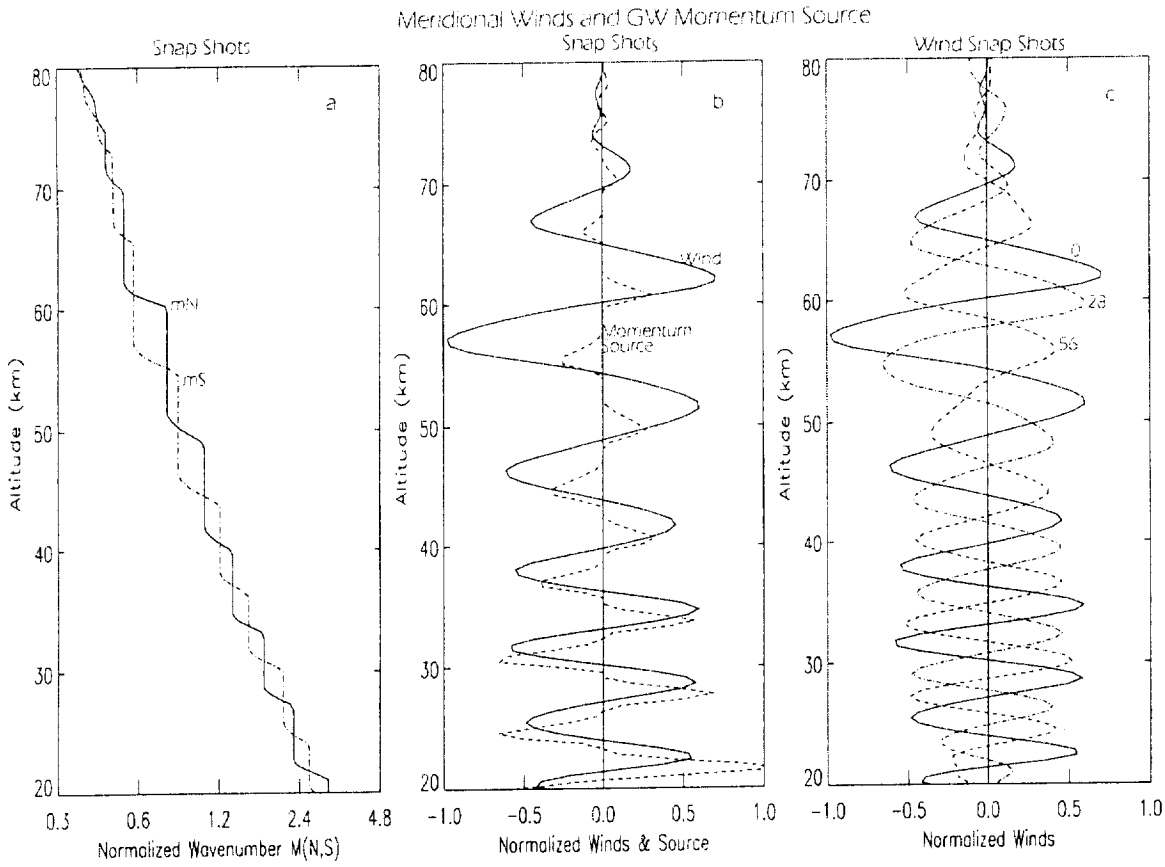
Meridional Winds and GW Momentum Source
Snap Shots
a
mN
mS
Altitude (km)
Normalized Wavenumber M(N,S)
Snap Shots
b
Wind
Momentum Source
Normalized Winds & Source
Wind Snap Shots
c
0
2a
5a
Normalized Winds

Figure 7

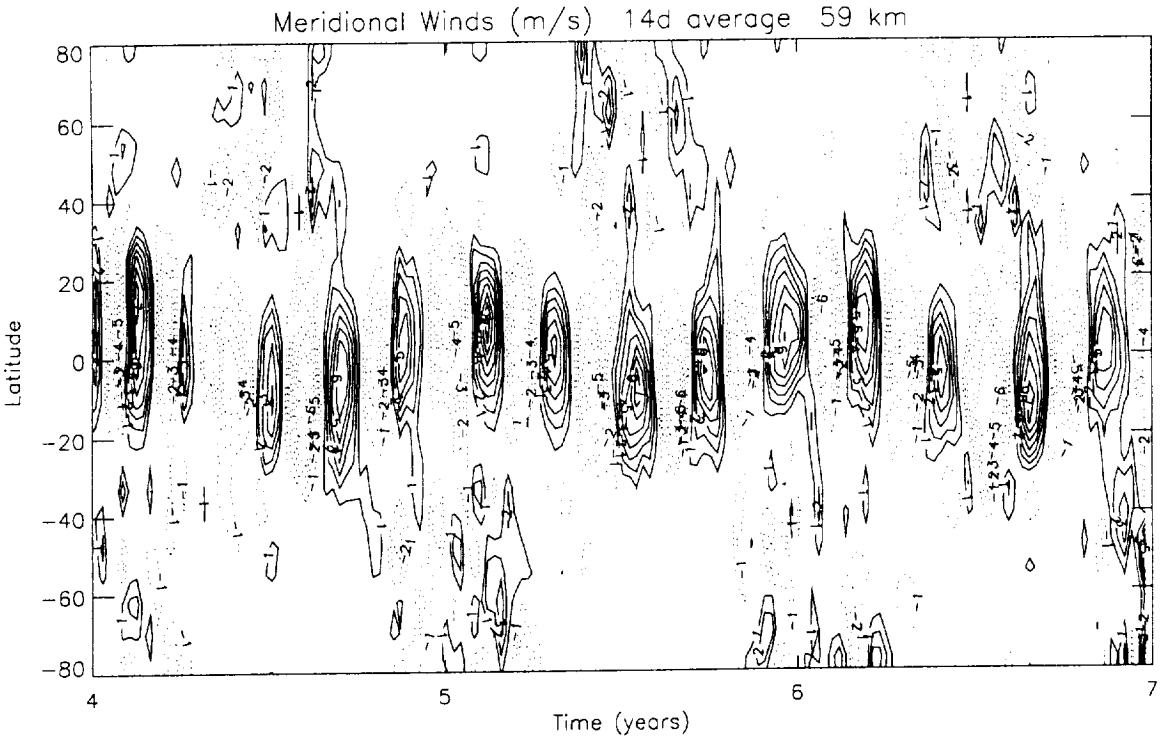
Meridional Winds (m/s) 14d average 59 km
Latitude
80
60
40
20
0
-20
-40
-60
-80
4
5
6
7
Time (years)

Figure 8

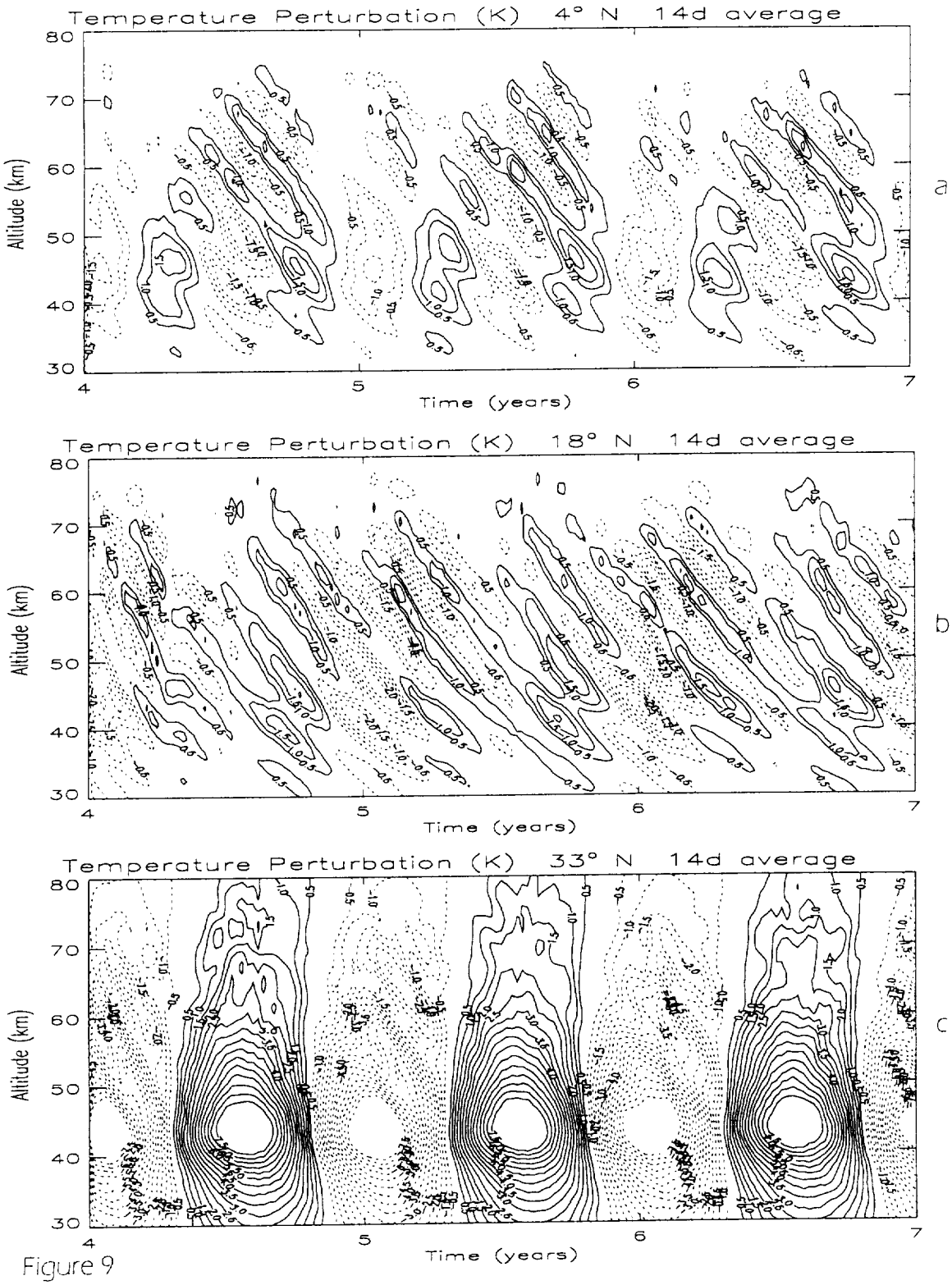
Temperature Perturbation (K) 4° N 14d average
Altitude (km)
Time (years)
a
Temperature Perturbation (K) 18° N 14d average
Altitude (km)
Time (years)
b
Temperature Perturbation (K) 33° N 14d average
Altitude (km)
Time (years)
c

Figure 9

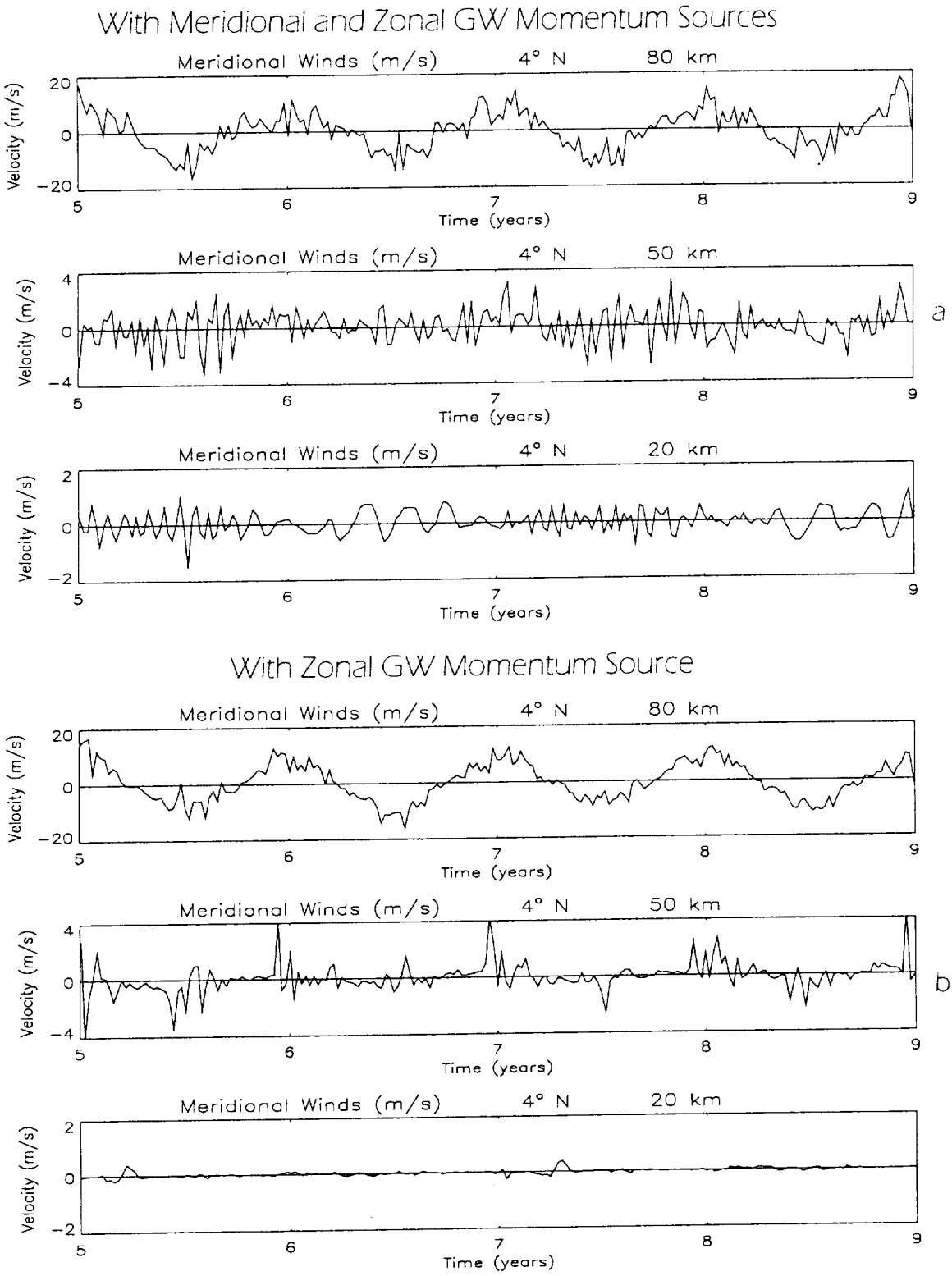
With Meridional and Zonal GW Momentum Sources
Meridional Winds (m/s) 4° N 80 km
Velocity (m/s)
20
0
−20
5
6
7
8
9
Time (years)
Meridional Winds (m/s) 4° N 50 km
Velocity (m/s)
4
0
−4
5
6
7
8
9
Time (years)
a
Meridional Winds (m/s) 4° N 20 km
Velocity (m/s)
2
0
−2
5
6
7
8
9
Time (years)
With Zonal GW Momentum Source
Meridional Winds (m/s) 4° N 80 km
Velocity (m/s)
20
0
−20
5
6
7
8
9
Time (years)
Meridional Winds (m/s) 4° N 50 km
Velocity (m/s)
4
0
−4
5
6
7
8
9
Time (years)
b
Meridional Winds (m/s) 4° N 20 km
Velocity (m/s)
2
0
−2
5
6
7
8
9
Time (years)

Figure 10

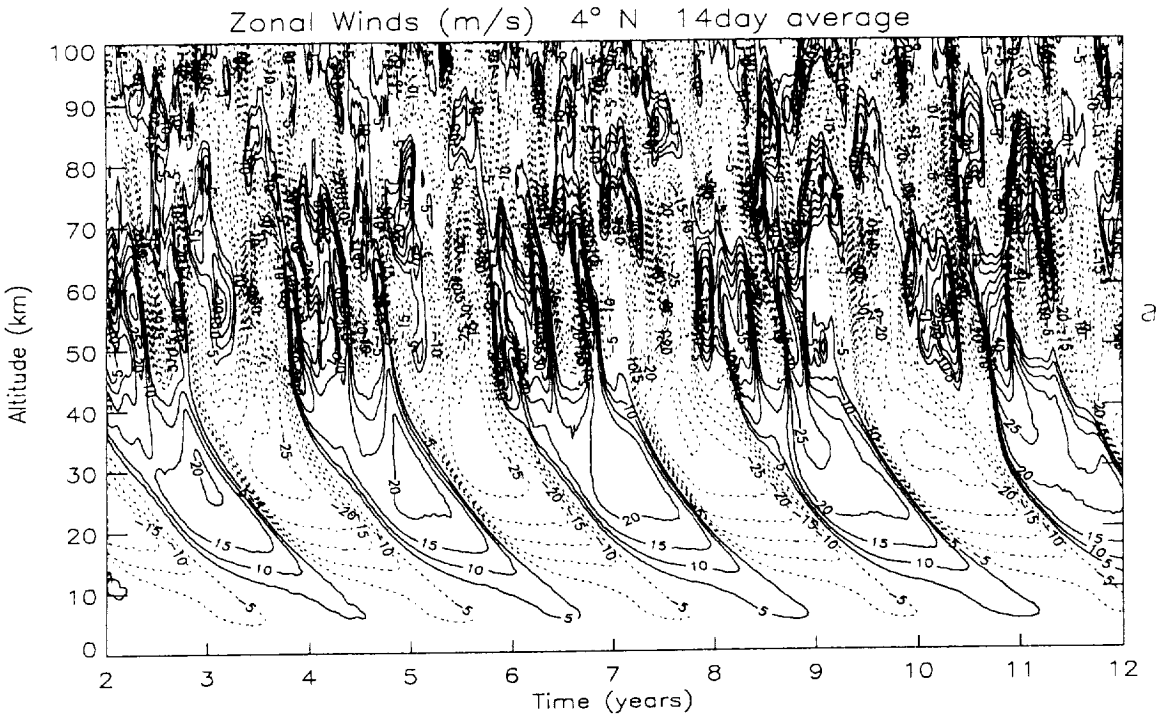
Zonal Winds (m/s) 4° N 14day average
Altitude (km)
Time (years)
a

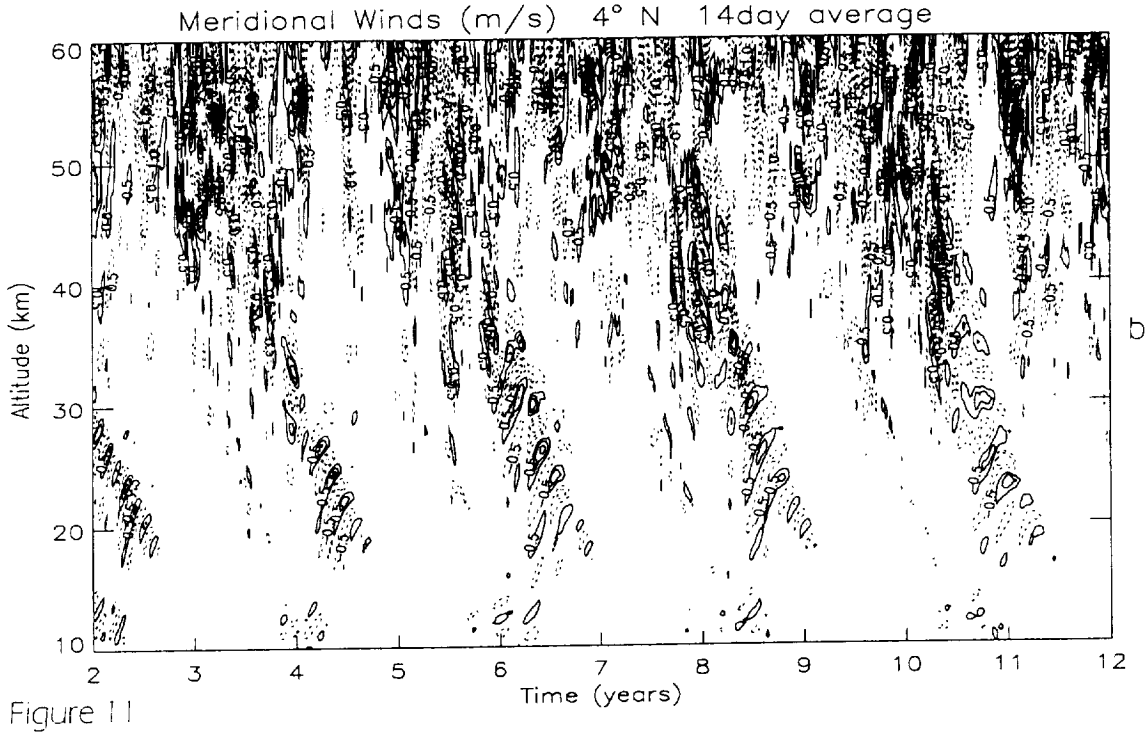
Meridional Winds (m/s) 4° N 14day average
Altitude (km)
Time (years)
b

Figure 11

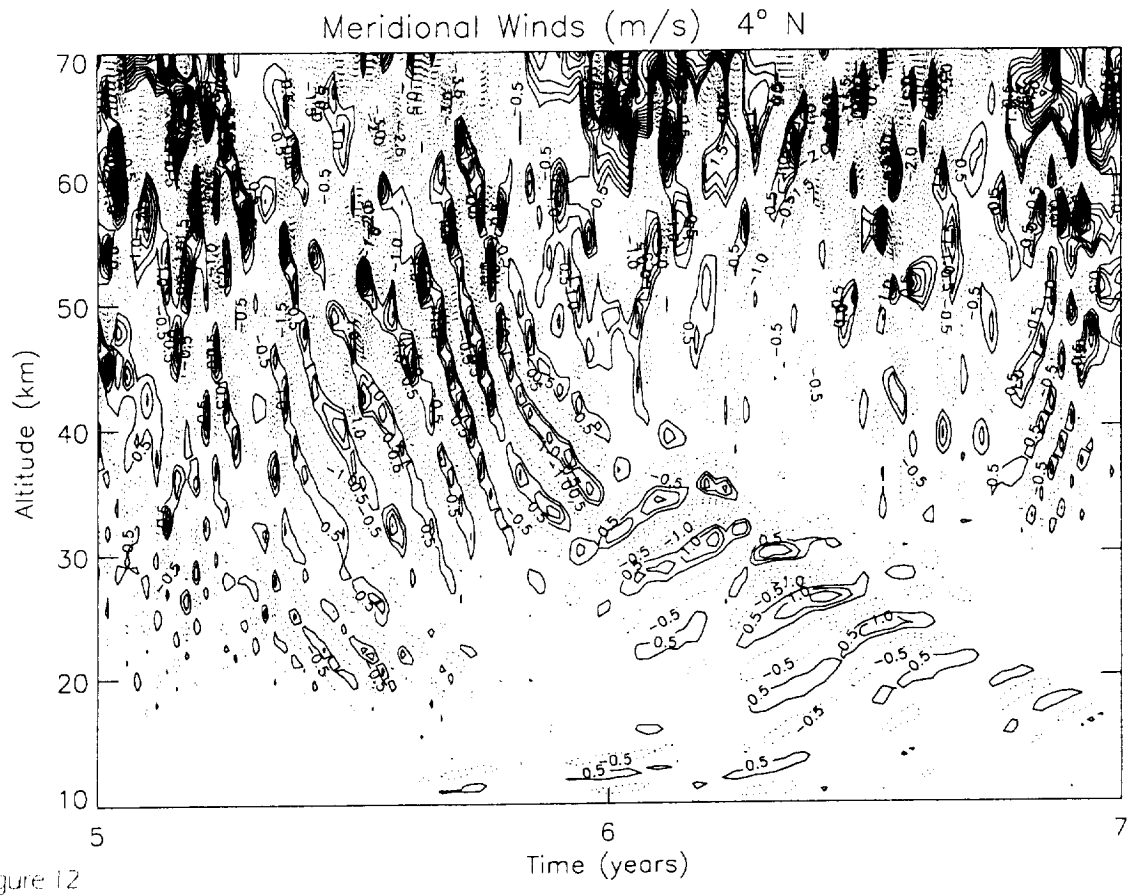
Meridional Winds (m/s) 4° N
Altitude (km)
70
60
50
40
30
20
10
5
6
7
Time (years)

Figure 12

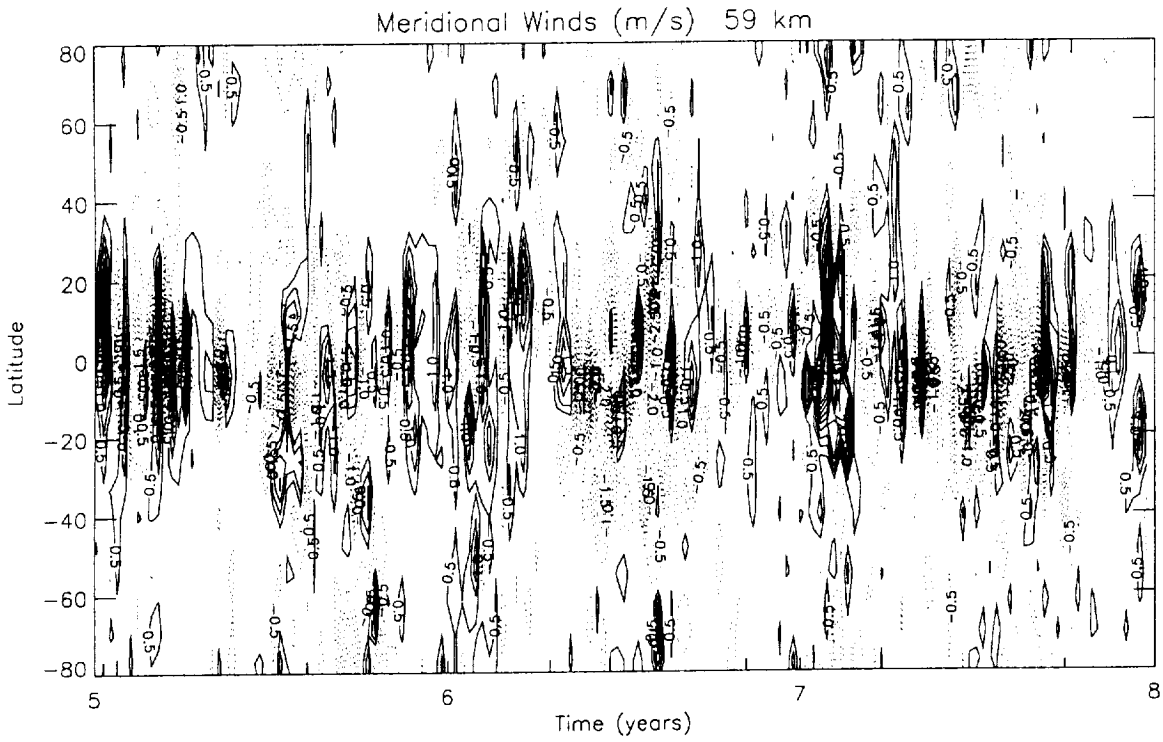
Meridional Winds (m/s) 59 km
Latitude
80
60
40
20
0
−20
−40
−60
−80
5
6
7
8
Time (years)

Figure 13

Interseasonal Variations in the Middle Atmosphere Forced by Gravity Waves

H. G. Mayr[1], J. G. Mengel[2], D. P. Drob[3], H. S. Porter[4], and K. L. Chan[5]
[1] Goddard Space Flight Center, Greenbelt, MD, 20771
[2] Science Systems & Applications, Inc., Lanham, MD,
[3] Naval Research Laboratory, Washington, DC, 20375
[4] Furman University, Greenville, SC, 29613
[5] Hong Kong University of Science and Technology, Hong Kong, China

Popular Summary:
Waves propagating in the east/west directions accelerate the axisymmetric (or zonal mean) component of the zonal winds to generate in the middle atmosphere, (a) the Quasi Biennial Oscillation (QBO) and Semiannual Oscillation (SAO) at low latitudes and (b) the anomalous seasonal variations with lower temperatures in summer than in winter at altitudes around 80 km. Applying Hines' Doppler Spread Parameterization for gravity waves (GWs), we have been able to model these dynamical features in our global-scale Numerical Spectral Model (NSM) that extends from the Earth's surface into the thermosphere. The zonal mean meridional winds are comparatively small, and their interactions with the waves therefore tend to be ignored. But we have carried out a study, which indicates that this wave interaction in fact may be important, for it can produce interseasonal variations in the middle atmosphere affecting the variations of the temperature and possibly ozone. Our analysis shows that GWs propagating in the north/south directions can generate meridional wind oscillations (MWO), which appear to be the counterpart to the QBO in the zonal winds. Like the QBO, the MWO is a wave driven non-linear oscillation, but its period is only on the order of months. We present numerical results from 2D and 3D versions of our model to elucidate some properties of the MWO, and a scale analysis serves to provide understanding.